*CORRESPONDENCE
Liying Ma
✉ 601763090@qq.com
Desheng Liu
✉ desheng_liu@sina.com

Alkaloid diversity expansion of a talent fungus *Penicillium raistrichii* through OSMAC-based cultivation

Meijia Zhong, Huihui Kang, Weizhong Liu, Liying Ma* and Desheng Liu*

Laboratory of Natural Drug Discovery and Research, College of Pharmacy, Binzhou Medical University, Yantai, China

Introduction: Alkaloidal natural products are attractive for their broad spectrum of pharmaceutical bioactivities. In the present work, the highly productive saline soil derived fungus, *Penicillium raistrichii*, was subjected to the strategy of OSMAC (one strain many compounds) with changes of cultivation status. Then, the work-flow led to the expansion of the alkaloid chemical diversity and subsequently induced the accumulation of four undescribed alkaloids, named raistrimides A−D (**1−4**), including three β-carbolines (**1−3**), one 2-quinolinone (**4**), and one new natural product, 2-quinolinone (**5**), along with five known alkaloid chemicals (**6−10**).

Methods: A set of NMR techniques including ^{1}H, ^{13}C, HSQC and HMBC, along with other spectroscopic data of UV-Vis, IR and HRESIMS, were introduced to assign the plain structures of compounds **1−10**. The absolute configuration of **1−3** were elucidated by means of X-ray crystallography or spectroscopic analyses on optical rotation values and experimental electronic circular dichroism (ECD) data. In addition, it was the first report on the confirmation of structures of **6**, **7** and **9** by X-ray crystallography data. The micro-broth dilution method was applied to evaluate antimicrobial effect of all compounds towards *Staphylococcus aureus*, *Escherichia coli*, and *Candida albicans*.

Results and discussion: The results indicated compounds **1**, **3** and **4** to be bioactive, which may be potential for further development of anti-antimicrobial agents. The finding in this work implied that OSMAC strategy was a powerful and effective tool for promotion of new chemical entities from *P. raistrichii*.

Introduction

It is clearly understood that the secondary metabolite (SM) production capacity of microbes lies on biosynthetic gene clusters (BGCs) (Bills and Gloer, 2016; Genilloud, 2019; Zhang J. J. et al., 2019; Ke and Yoshikuni, 2020; Alexander, 2023). Yet, the traditional workflow involving laboratory cultivation of microbes, followed by extraction of fermentation, SMs purification, and structure elucidation, often results in the silent or weak expression of BGCs and thus confines the occurrences and number of the new chemical entities, due to failure of resembling the nature environment with intense microbial competition. There is a growing consensus that unlocking the silent BGCs is a key channel to counteract the dramatic decline in the quantity of novel naturally-produced chemical structures (Reen et al., 2015; Zhang X. et al., 2019).

During the recent several decades, in order to tap the biosynthetic potential and strengthen silent gene expression, molecular methodologies (Reen et al., 2015; Palys et al., 2020; Wang et al., 2020; Han et al., 2020a,b) like gene manipulation, including knocking down, introduction or heterologous expression, regulation of promoters, and induction of mutations, as well as approaches based on cultivation conditions variation, have been employed and have achieved great successes in mining cryptic SMs. Of these, the one strain many compounds (OSMAC) strategy, covering medium variation, cultivation condition change, co-cultivation, or addition of epigenetic modifiers, has been efficiently applied to promote new therapeutic agents discovery, highlighting it as an easy and productive approach to trigger the reaction of the crypt BGCs and enhance the natural SMs production according to the extensive literature reports (Bode et al., 2002; Romano et al., 2018; Pan et al., 2019).

During our ongoing efforts in pursuit of therapeutic pharmaceuticals from saline soil-derived fungi, a talent genus *P. raistrichii* isolated from saline sediment in Bohai Bay, entered into our vision. Chemical investigations on the metabolic profile resulted in the discovery of several different novel scaffolds including polyketides and alkaloids with biological behaviors of antiinsectan, antimicrobial, radical scavenging, cytotoxic, or anti-HCV activities (Belofsky et al., 1998; Ma et al., 2016; Jia et al., 2017; Liu et al., 2018; Li et al., 2019). In recognition of the superior ability for the production of intriguing molecules from the talent strain, and also enlightened by OSMAC strategy of expansion on the fungal metabolome, the strain was subjected to culture under static conditions in a liquid medium. Excitingly, the change of culture conditions, which may have exerted influences on the biochemical reactions, caused the strain to produce four new alkaloids, named raistrimides A-D (**1–4**), one new natural product 2-quinolinone, 3-hydroxy-4-(4′-methoxyphenyl)-2(1H)-quinolinone (**5**) (He et al., 2015), and five known alkaloids, pesimquinolone R (**6**) (Dai et al., 2021), peniprequinolone (**7**) (Hayashi et al., 1997; Uchida et al., 2006), 4,5-dihydroxy-3,4-dihydro-3-methoxy-4-(4′-methoxyphenyl)-2(1H)-quinolinone (**8**) (Framm et al., 1973), dehydrocyclopeptin (**9**) (Ishikawa et al., 2014), and tunicoidine F (**10**) (Wen et al., 2014; Zhang et al., 2015). Detailed information about the isolation, purification, and structure elucidation, as well as the antimicrobial effect assessment of these compounds (Figure 1) is presented in this work.

Materials and methods

General experimental procedures

An uncorrected XRC-1 micro melting point apparatus was used to measure the melting points. Uv–Vis and IR data were performed on a TU-1091 spectrophotometer and a Thermo Nicolet 6,700 infrared spectrophotometer, respectively. A Rudolph Autopol V Plus digital polarimeter, a Bruker Smart 1,000 CCD X-ray diffractometer, and an Applied Photophysics Chirascan spectropolarimeter were used for the determination of optical rotations, X-ray crystal data, and electron circular dichroism (ECD) spectra, respectively. Varian Inova 600 and Bruker AV-400/AVIII 500 spectrometers were used to measure 1D and 2D NMR data in different deuterium solvents using tetramethylsilane as an internal standard (IS). HRESIMS spectra were recorded using an Agilent 1200RRLC-6520 Accurate-Mass Q-TOF

LC/MS mass spectrometer or a Waters Q-TOF Ultima GLOBAL GAA076 LC. A Shimadzu LC-6 AD and LC-20A Liquid Chromatography were applied for the preparative isolation and analysis on HyperClone C_{18} columns (5 μm, 10×250 mm, 5 μm, 4.6×250 mm, respectively). Open column chromatography (CC) isolations were performed on silica gel (200–300 mesh, Qingdao Marine Chemical, China), reverse phase (RP) C_{18} material (Pharmacia Fine Chemical Co., Sweden), and Sephadex LH-20 (Ge Healthcare Bio-Sciences AB, Sweden).

Fungal material

Saline soil samples were collected from the coast in the Circum-Bohai-Sea region in Zhanhua county, from which a talent strain of *Penicillium raistrickii* with GenBank Accession NO. HQ717799 was isolated in August 2008. The voucher specimen was preserved at the laboratory of Natural Drug Discovery and Research, Binzhou Medical University.

Cultivation and extraction

The spores of *P. raistrickii* growing well on potato dextrose agar (PDA) were incubated in 500-mL Erlenmeyer flasks which contained 180 mL of culture medium comprising 2% glucose, 1% maltose, 0.03% yeast extract, 0.003% $MgSO_4 \cdot 7H_2O$, and 0.005% KH_2PO_4 with the natural pH value in seawater gathered from offshore areas near Yantai, and fermented under static condition at about 28°C for 60 days. A whole volume of 40 L culture broth was isolated into supernatant and mycelia through cheesecloth. The supernatant was extracted with ethyl acetate (3×30 L), and the mycelia was extracted with methanol (3×10 L) to afford crude aqueous extract followed by partitioning with ethyl acetate, which yielded an extract of 45 g.

Isolation and purification

The whole extract was subjected to a VLC column with silica gel eluting by a step gradient of petroleum ether/CHCl₃ (from 1:2 to 0:1, v/v) to give five fractions (Fr.s 1–5), and then followed by a step gradient of CHCl₃/MeOH (from 1:2 to 0:1, v/v) to afford another five fractions (Fr.s 6–10). Among these, Fr. 3 (4.1 g) and Fr. 4 (3.3 g) were separated with MeOH/H₂O (20:80 to 100:0, v/v) on ODS to afford nine (Fr.s 3.1–3.9) and six (Fr.s 4.1–4.6) subfractions, respectively. Then, compound **1** (9.2 mg) was purified by a Sephadex LH-20 CC from Fr. 4.3 (0.2 g) with MeOH as the eluent. Compounds **2** (3.6 mg) and **10** (16.0 mg) were purified by semipreparative HPLC (MeOH:H₂O, 70:30, v:v) with a retention time (t_R) of 20.8 min and 17.3 min, respectively. Compound **3** (22.0 mg) was also obtained from semipreparative HPLC (MeOH:H₂O, 65:35, v:v) with a t_R value of 17.1 min. Compounds **4** (12.6 mg) and **5** (9.3 mg) were given from Fr. 3.8 (0.5 g) which was chromatographed on a silica gel column, eluting with CHCl₃/MeOH (30:1, v/v). Compounds **6** (14.6 mg) and **8** (32.6 mg) were obtained from Fr. 4.2 (0.7 g) and Fr. 5 (1.7 g) by crystalization in MeOH. Compounds **7** (15.8 mg) and **9** (10.8 mg) were purified by semipreparative HPLC (MeOH:H₂O, 60:70, v:v) from Fr. 3.3 (0.9 g) and Fr. 4.6 (0.7 g) with values of 26.2 min and 13.8 min, respectively.
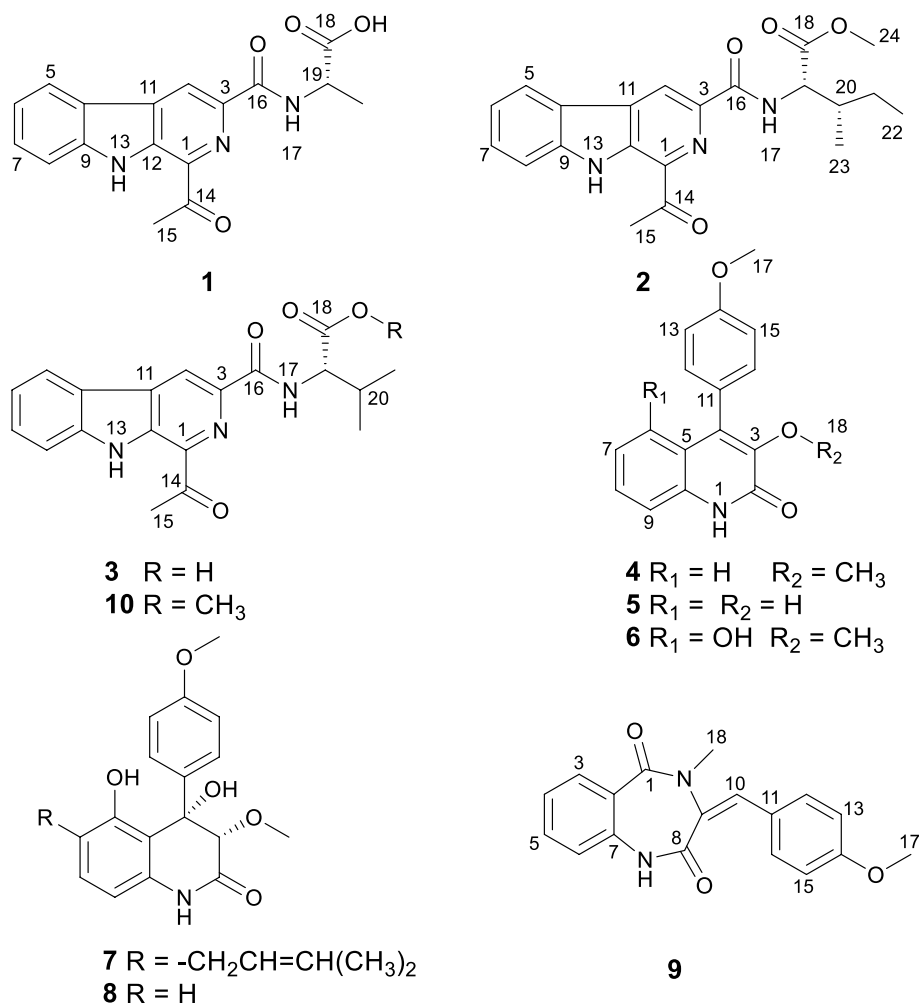
FIGURE 1
Chemical structures of compounds **1–10**.

Raistrimide A (1)

Yellowish needle (MeOH); mp 278°C (dec.); UV (MeOH) λ_{max} (log ε): 377 (3.79), 286 (4.61), 220 (4.56) nm; IR (ATR) ν_{max} 3,352, 2,869, 1,728, 1,633, 1,537, 1,493, 1,444, 1,336, 1,195, 1,115, 963, 887, 750, 682 cm^{-1}; ^{1}H and ^{13}C NMR data, see Table 1; HRESIMS (m/z): 324.0993 [M – H]$^-$ (calcd for $C_{17}H_{14}N_3O_4$, 324.0990). $[\alpha]_D^{20}$ + 10.8 (c 0.062, MeOH); ECD (MeOH) λ_{max} ($\Delta\varepsilon$) 229 (− 45.21), 204 (+ 120.47) nm.

Raistrimide B (2)

yellowish needle (MeOH); mp 196–199°C; UV (MeOH) λ_{max} (log ε): 377 (3.67), 287 (4.53), 220 (4.44) nm; IR (ATR) ν_{max} 3,329, 2,964, 1,740, 1,663, 1,626, 1,515, 1,491, 1,459, 1,204, 1,179, 963, 847, 738, 683 cm^{-1}; ^{1}H and ^{13}C NMR data, see Table 1; HRESIMS (m/z): 382.1762 [M + H]$^+$ (calcd for $C_{21}H_{24}N_3O_4$, 382.1761). $[\alpha]_D^{20}$ + 4.4 (c 0.069, MeOH); ECD (MeOH) λ_{max} ($\Delta\varepsilon$) 280 (+ 0.88), 268 (− 0.02), 240 (+ 0.84), 229 (− 0.50), 204 (+ 3.99) nm.

Raistrimide C (3)

yellowish needle (MeOH); mp 280°C (dec.); UV (MeOH) λ_{max} (log ε): 377 (3.73), 286 (4.53), 220 (4.46) nm; IR (ATR) ν_{max} 3,394, 2,969,

2,542, 1,745, 1,680, 1,622, 1,542, 1,494, 1,361, 1,302, 1,202, 1,147, 965, 899, 788, 742, 681 cm^{-1}; ^{1}H and ^{13}C NMR data, see Table 1; HRESIMS (m/z): 352.1302 [M – H]$^-$ (calcd for $C_{19}H_{18}N_3O_4$, 352.1303). $[\alpha]_D^{20}$ + 12.0 (c 0.055, MeOH); ECD (MeOH) λ_{max} ($\Delta\varepsilon$) 280 (+ 0.73), 264 (− 0.24), 232 (+ 0.30), 224 (− 0.21), 204 (+ 3.68) nm.

Raistrimide D (4)

colorless needle (MeOH); mp 230–232°C; UV (MeOH) λ_{max} (log ε): 337 (3.18), 324 (3.36), 311 (3.35), 298 (3.33), 278 (3.37), 218 (4.03) nm; IR (ATR) ν_{max} 1,647, 1,609, 1,553, 1,515, 1,500, 1,434, 1,282, 1,219, 1,175, 1,146, 1,017, 899, 836, 747, 699 cm^{-1}; ^{1}H and ^{13}C NMR data, see Table 2; HRESIMS (m/z): 280.0973 [M – H]$^-$ (calcd for $C_{17}H_{14}NO_3$, 280.0968).

3-hydroxy-4-(4′-methoxyphenyl)-2(1H)-quinolinone (5)

Colorless blocks (MeOH); UV (MeOH) λ_{max} (log ε): 331 (3.51), 318 (3.65), 306 (3.60), 286 (3.58), 243 (3.86), 222 (4.16) nm; IR (ATR) ν_{max} 2,918, 1,652, 1,608, 1,574, 1,515, 1,501, 1,455, 1,403, 1,291, 1,245, 1,031, 950, 881, 753, 713 cm^{-1}; ^{1}H and ^{13}C NMR data, see Table 2; HRESIMS (m/z): 266.0815 [M – H]$^-$ (calcd for $C_{16}H_{12}NO_3$, 266.0812).

TABLE 1 ^{1}H and ^{13}C NMR data for 1−3 (DMSO-d_6).

NO.	1[a]		2[b]		3[a]	
	δ_C, Type	δ_H, mult (J Hz)	δ_C, Type	δ_H, mult (J Hz)	δ_C, Type	δ_H, mult (J Hz)
1	134.0, C		134.4, C		133.9, C	
3	138.1, C		138.0, C		137.7, C	
4	118.1, CH	9.11, s	118.5, CH	9.11, s	118, CH	9.12, s
5	122.3, CH	8.46, d (7.5)	122.8, CH	8.47, d (7.5)	122.4, CH	8.47, d (7.7)
6	120.9, CH	7.35, t (7.5)	121.3, CH	7.36, t (7.5)	120.9, CH	7.36, t (7.7)
7	129.4, CH	7.64, dd (8.2, 7.5)	129.9, CH	7.64, dd (8.2, 7.5)	129.4, CH	7.65, dd (8.2, 7.7)
8	113.3, CH	7.85, d (8.2)	113.8, CH	7.84, d (8.2)	113.4, CH	7.85, d (8.2)
9	142.4, C		142.8, C		142.4, C	
10	120.3, C		120.7, C		120.3, C	
11	132.0, C		132.5, C		132.1, C	
12	134.9, C		135.4, C		134.9, C	
13		12.23, s		12.26, s		12.26, s
14	200.9, C		200.9, C		200.4, C	
15	25.9, CH$_3$	2.93, s	26.2, CH$_3$	2.90, s	25.6, CH$_3$	2.90, s
16	163.7, C		164.4, C		163.9, C	
17		8.85, d (7.5)		8.65, d (8.3)		8.59, d (8.7)
18	174.0, C		172.3, C		172.8, C	
19	47.9, CH	4.59, m	56.8, CH	4.60, dd (8.3, 5.2)	57.1, CH	4.52, dd (8.7, 4.9)
20	17.7, CH$_3$	1.52, d (7.1)	37.2, CH	2.10, m	30.5, CH	2.34, m
21			25.4, CH$_2$	1.54, m; 1.31, m	19.2, CH$_3$	1.03, d (6.6)
22			16.6, CH$_3$	0.95, t (6.7)	17.7, CH$_3$	1.03, d (6.6)
23			11.7, CH$_3$	0.98, d (7.0)		
24			52.5, CH$_3$	3.73, s		
OH		12.89, br s				13.07, s

[a][1]H (400 MHz) and [13]C (100 MHz). [b][1]H (600 MHz) and [13]C (150 MHz).

Dehydrocyclopeptin (9)

colorless blocks (MeOH); 97–99°C; UV (MeOH) λ_{max} (log ε): 288 (4.28), 214 (4.59), 220 (4.46), 205 (4.43) nm; IR (ATR) ν_{max} 3,064, 1,670, 1,622, 1,602, 1,512, 1,478, 1,385, 1,252, 1,175, 1,028, 825, 754, 699 cm^{-1}; ^{1}H and ^{13}C NMR data, see Table 3.

X-ray single-crystal structure determinations of 2, 4, 6, 7, and 9

All of the determined compounds were acquired from the solvent of MeOH by vapor diffusion. The structure elucidation of these compounds was settled by the Sheldrick (2014) software package through direct methods and were refined using least squares minimization. The crystallographic data of compounds **2** (CCDC 2002826), **4** (CCDC 2002827), **6** (CCDC 2002870), **7** (CCDC 2002825), and **9** (CCDC 2002821) have already been deposited in the Cambridge Crystallographic Data Centre.[1]

Crystal data for 2

$C_{21}H_{23}N_3O_4$, $M_r = 381.42$, monoclinic, space group C2, $a = 15.8834$ (11) Å, $b = 6.8528$ (7) Å, $c = 18.4959$ (17) Å, $V = 2013.0$ (3) Å^3, $T = 293$ (2) K, $Z = 4$, μ(Cu Kα) = 0.723 mm^{-1}, $D_{calcd} = 1.259$ g/cm^3. $\alpha = \gamma = 90°$, $\beta = 90.565$ (8)°. In total, 3,289 reflections were measured (9.56 ≤ 2θ ≤ 132.08), with 2,354 independent unique reflections ($R_{int} = 0.0466$). The final refinement [I ≥ 2σ (I)] gave $R_1 = 0.0633$ and $wR_2 = 0.1351$. The final refinement presented $R_1 = 0.1103$ and $wR_2 = 0.1650$ (all data). Flack parameter = 0.0 (9).

Crystal data for 4

$C_{17}H_{15}NO_3$, $M_r = 281.30$, monoclinic, space group C2/c, $a = 26.002$ (2) Å, $b = 7.4221$ (8) Å, $c = 14.8450$ (13) Å, $V = 2787.6$ (4) Å^3, $T = 293$ (2) K, $Z = 8$, μ(Cu Kα) = 0.092 mm^{-1}, $D_{calcd} = 1.341$ g/cm^3. $\alpha = \gamma = 90°$, $\beta = 103.343$ (2)°. In total, 5,145 reflections were measured (5.64 ≤ 2θ ≤ 50.02), with 2,453 independent unique reflections ($R_{int} = 0.1063$). The final refinement [I ≥ 2σ (I)] gave $R_1 = 0.1063$, and $wR_2 = 0.1351$. The final refinement presented $R_1 = 0.0951$ and $wR_2 = 0.1400$ (all data).

Crystal data for 6

$C_{17}H_{15}NO_4$, $M_r = 297.30$, monoclinic crystal, space group P2$_1$/n, $a = 8.7113$ (5) Å, $b = 9.5303$ (7) Å, $c = 17.3892$ (12) Å, $\alpha = \gamma = 90°$,

---

1 www.ccdc.cam.ac.uk/data_request/cif

TABLE 2 ^{1}H and ^{13}C NMR data for 4 (Py-d_5) and 5 (DMSO-d_6).

NO.	4[a]		5[b]	
	δ_C, Type	δ_H, mult (J Hz)	δ_C, Type	δ_H, mult (J Hz)
1		13.28, s		12.20, s
2	160.3*, C		158.3, C	
3	147.0, C		142.5, C	
4	138.3, C		121.1, C	
5	121.8, C		125.6, C	
6	127.3, CH	7.39, d (8.0)	126.3, CH	7.33, overlapped
7	122.5, CH	7.15, dd (8.0, 7.5)	122.0, CH	7.12, overlapped
8	129.2, CH	7.48, dd (8.0, 7.5)	124.4, CH	7.12, overlapped
9	115.7, CH	7.60, d (8.0)	115.2, CH	7.33, overlapped
10	137.5, C		133.2, C	
11	126.9, C		123.7, C	
12/16	131.6	7.44, d (8.5)	131.1	7.27, d (8.3)
13/15	114.8	7.18, d (8.5)	113.8	7.07, d (8.3)
14	160.2*, C		158.7, C	
17	55.7, CH$_3$	3.78, s	55.1, CH$_3$	3.83, s
18	60.3, CH$_3$	4.05, s		
OH				9.12, s

[a]^{1}H (500 MHz) and ^{13}C (125 MHz). [b]^{1}H (400 MHz) and ^{13}C (100 MHz). *Assignments interchangeable.

TABLE 3 ^{1}H (400 MHz) and ^{13}C (100 MHz) NMR data for 9 (Acetone-d_6).

NO.	δ_C, Type	δ_H, mult (J Hz)	NO.	δ_C, Type	δ_H, mult (J Hz)
1	167.2, C		9	133.4, C	
2	126.9, C		10	130.5, C	
3	131.9, CH	7.88, d (7.2)	11	125.9, C	
4	125.0, CH	7.24, overlapped	12/16	132.0	7.39, d (8.7)
5	133.3, CH	7.51, t (7.2)	13/15	115.4	7.01, d (8.7)
6	121.5, C	7.24, overlapped	14	161.7, C	
7	137.8, C		17	55.8, CH$_3$	3.84, s
8	171.5, C		18	35.5, CH$_3$	3.13, s

$\beta = 103.465$ (2)°, $V = 1403.99$ (16) Å^3, $T = 293$ (2) K, $Z = 4$, μ(Cu Kα) = 0.834 mm^{-1}, D_{calc} = 1.407 g/cm^3. In total, 4,326 reflections were measured (10.46 $\leq 2\theta \leq$ 132.18), with 2,454 independent unique reflections (R_{int} = 0.0221). The final refinement [I $\geq 2\sigma$ (I)] gave R_1 = 0.0483, and wR_2 = 0.1334. The final refinement presented R_1 = 0.0608 and wR_2 = 0.1451 (all data).

Crystal data for 7

C$_{22}$H$_{24}$NO$_5$, M_r == 382.42, orthorhombic crystal, space group P2$_1$2$_1$2$_1$, a = 9.6170 (4) Å, b = 13.3217 (5) Å, c = 15.7153 (6) Å, $\alpha = \beta = \gamma = 90°$, $V = 2013.36$ (14) Å^3, $T = 293$ (2) K, $Z = 4$, μ(Cu Kα) = 0.732 mm^{-1}, D_{calc} = 1.262 g/cm^3. In total, 4,449 reflections

were measured (8.70 $\leq 2\theta \leq$ 132.78), with 2,991 independent unique reflections (R_{int} = 0.0261). The final refinement [I $\geq 2\sigma$ (I)] gave R_1 = 0.0498, and wR_2 = 0.1377. The final refinement gave R_1 = 0.0538, and wR_2 = 0.1422 (all data). Flack parameter = −0.27 (18).

Crystal data for 9

C$_{18}$H$_{16}$N$_2$O$_3$, M_r = 308.33, orthorhombic crystal, space group Pbca, a = 15.8992 (14) Å, b = 8.5824 (8) Å, c = 23.758 (2) Å, $\alpha = \beta = \gamma = 90°$, $V = 3241.8$ (5) Å^3, $T = 298$ (2) K, $Z = 8$, μ(Mo Kα) = 0.087 mm^{-1}, D_{calc} = 1.263 g/cm^3. In total, 14,810 reflections were measured (5.12 $\leq 2\theta \leq$ 50.04), with 2,861 independent unique reflections (R_{int} = 0.0842). The final refinement [I $\geq 2\sigma$ (I)] gave R_1 = 0.0516, and wR_2 = 0.1024. The final refinement presented R_1 = 0.1094 and wR_2 = 0.1146 (all data).

Biological assay

The antimicrobial activity of the isolated compounds was examined by the broth microdilution method according to the method as previously described (Ma et al., 2019). Microorganisms evaluated in this work included *Staphylococcus aureus*, *Escherichia coli*, and *Candida albicans*, and chloramphenicol or ketoconazole was applied as positive control.

Results and discussion

Compound **1** was obtained as a yellowish needle. The molecular formula of C$_{17}$H$_{15}$N$_3$O$_4$ was established from the deprotonated-ion HRESIMS at *m/z* 324.0993 (calcd for C$_{17}$H$_{14}$N$_3$O$_4$, 324.0990). It indicated a β-carboline chromophore by the feature of the UV absorptions at 377, 286 and 220 nm (Chen et al., 2010). The ^{1}H NMR spectrum in Table 1 showed four aromatic hydrogen signals at δ_H 8.46 (d, J = 7.5 Hz), 7.85 (d, J = 8.2 Hz), 7.64 (t, J = 7.5 Hz), and 7.35 (t, J = 7.5 Hz). The coupling patterns of these four aromatic hydrogens indicated the characteristics of an *o*-disubstituted benzene ring in the indole moiety (Tangella et al., 2018). The doublet methyl at δ_H 1.52, multiplet methine at δ_H 4.59, and the doublet imino proton at δ_H 8.85 were suggestive of an alanine residue functionality. The ^{13}C NMR data showed eleven aromatic carbon signals from δ_C 142.4 to 113.3 (Table 1), which featured the β-carboline skeleton. The signals of keto carbonyl at δ_C 200.9 and the methyl at $\delta_{C/H}$ 25.9/2.93, along with the HMBC crosspeaks from the methyl to the carbonyl, implied the existence of an acetyl group (Figure 2). It was located at C-1 on the basis of correlation from H-15 to C-1. Further interactions from H-17 to C-16 and C-19, and from H-4 to C-16 suggested the linkage of C-3 and the alanine residue through C-16. Thus, the plain structure of **1** was accomplished. Considering that alanine moiety plays a crucial role in the specific optical rotation in compound **1** (the same condition also applied to compounds **2**, **3**, and **10**), the consistent specific rotation behaviors of **1** {[α]$_D^{20}$ + 10.8 (*c* 0.062, MeOH)} and oldhamiaine A {[α]$_D^{25}$ + 14.0 (*c* 0.062, MeOH)} suggested the absolute configuration of C-19 to be *S* (Zhang et al., 2015). Additionally, the experimental and calculated ECD curves (Figure 3) further supported the absolute configuration assignment. The absolute stereochemistry of **1** was established to be 19*S*.
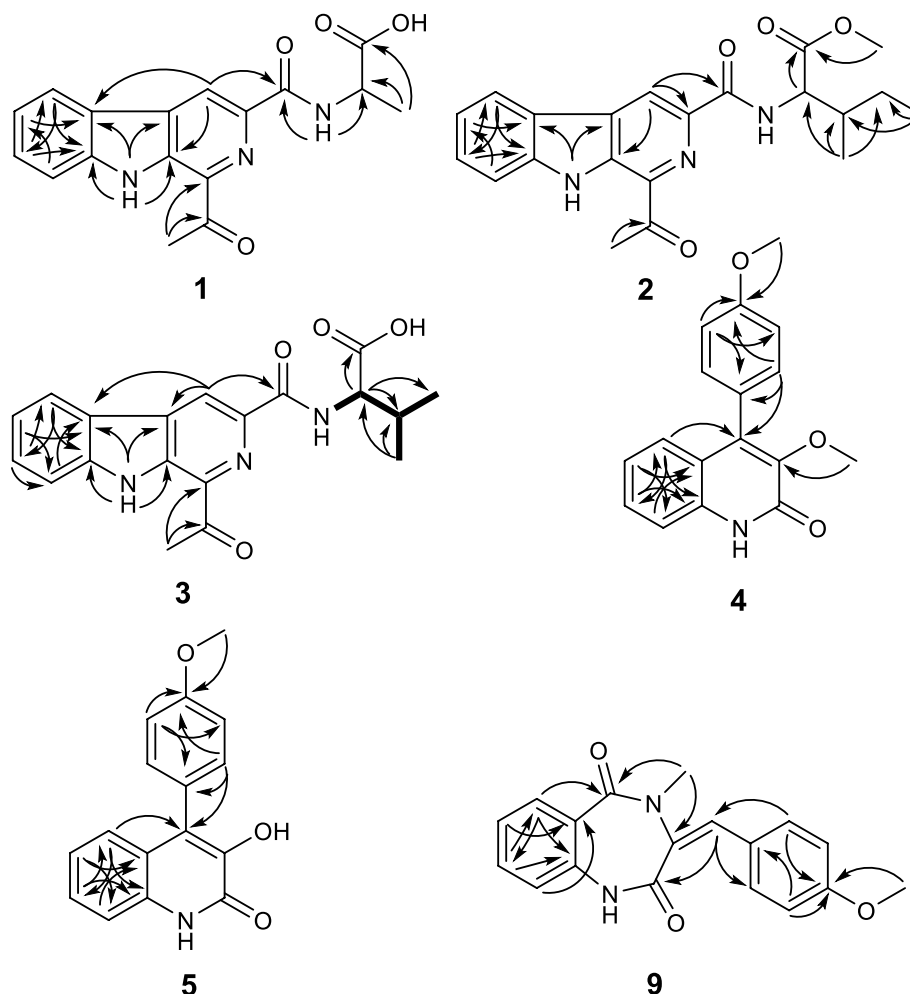
FIGURE 2
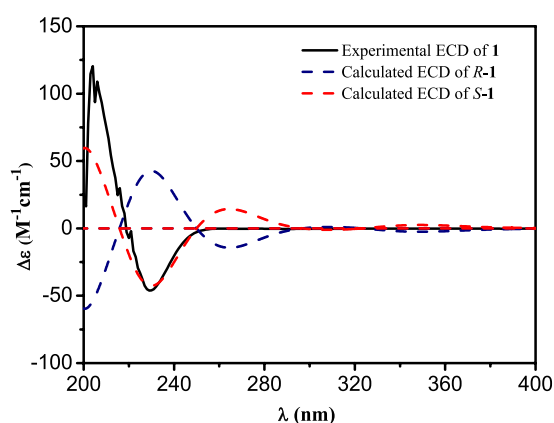Key HMBC correlations of **1–5** and **9**, and key COSY for **3**.

FIGURE 3
Experimental and calculated ECD spectra of compound **1**.

Compound **2** was purified as light yellow needles with a molecular formula of $C_{21}H_{23}N_3O_4$ given by the positive HRESIMS at m/z 382.1762 $[M + H]^+$ (calcd for $C_{21}H_{24}N_3O_4$, 382.1761). The UV

and IR spectra of **2** also showed the absorption features of a β-carboline skeleton. The ^1H and ^{13}C NMR spectroscopic data of **2** (Table 1) in the downfield regions were almost identical with those of **1**, indicative of the same β-carboline moiety. Furthermore, the signals in the upfield of two methines at δ_H 4.60 and 2.10, one diastereotopic methylene at δ_H 1.54 and 1.31, two methyls at δ_H 0.98 and 0.95, and the carbon resonances at δ_C 56.8, 37.2, 25.4, 16.6, 11.7 (Table 1), suggested the fragment of an isoleucine residue, which was supported by the HMBC correlations (Figure 2). Finally, the X-ray analyses unambiguously determined the absolute configuration of **2** (Figure 4).

Compound **3**, light yellow needles, was determined to have a molecular formula of $C_{19}H_{19}N_3O_4$ by the negative HRESIMS data (m/z 352.1302, calcd for $C_{19}H_{18}N_3O_4$, 352.1303). Its UV and IR absorption bands were almost the same as those of compounds **1** and **2**. The spectroscopic data covering ^1H and ^{13}C NMR (Table 1) closely resembled those of **1**, except for additional appearances of one methine and one methyl signals. Careful analyses of the chemical shifts and the splitting behaviors of a double doublets methine at δ_H 4.52, a multiplet methine at δ_H 2.34, two doublet methyl groups at δ_H 1.03, and a doublet NH at δ_H 8.59 were suggestive of a valine motif, which was supported by the corresponding ^1H-^1H COSY data
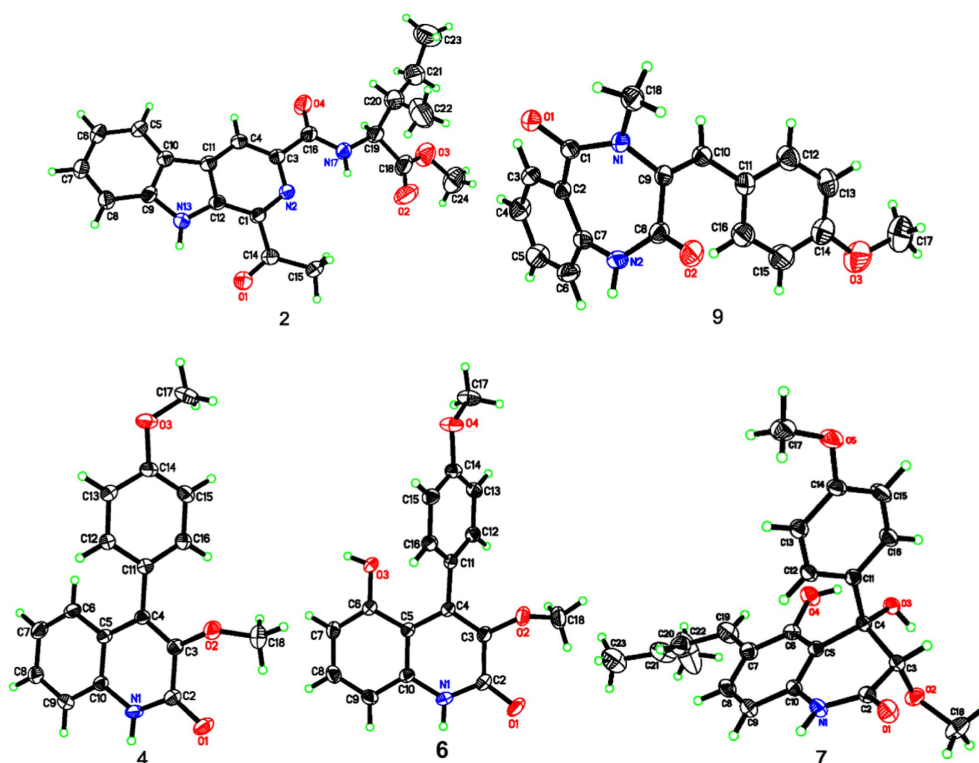
FIGURE 4
X-ray ORTEP diagrams of **2**, **4**, **6**, **7**, and **9**.

(Figure 2). The position of the valine motif was accomplished according to the HMBC interactions from H-4 and H-17 to C-16 (Figure 2). The acetyl group linked at C-1 was elucidated by the correlations from H-15 to C-1 and C-14. The similar ECD absorptions (ESI Supplementary Figure S24) together with evidence of the same optical rotation direction with that of **10** confirmed the absolute configuration of **3**.

Compound **4**, colorless needles, exhibited a deprotonated ion signal at *m/z* 280.0973 (calcd for $C_{17}H_{14}NO_3$, 280.0968) in negative HRESIMS, which corresponded with its molecular formula of $C_{17}H_{15}NO_3$. In ¹H NMR spectroscopic data, two aromatic protons at δ_H 7.44 and 7.18 (Table 2) which were presented in an *ortho*-coupled doublet fashion, indicated the presence of a *p*-disubstituted ring fragment. Four aromatic protons at δ_H 7.60, 7.48, 7.39, and 7.15 (Table 2) represented the existence of an *o*-disubstituted phenyl ring moiety. Evidence of the HMBC data from H-17 to C-14 and from H-12 to C-4 and C-14 revealed the methoxyl and C-4 anchored at the *p*-disubstituted phenyl ring (Figure 2). The NH group and C-4 were located at the *o*-disubstituted phenyl ring, which was supported by HMBC cross peaks from H-6 to C-4 and C-10, along with the chemical shift of C-10. The remaining three carbon signals, including a carbonyl at δ_C 160.3, a quaternary carbon at δ_C 147.0, and a methoxyl at δ_C 60.3 (Table 2) were assembled to complete the whole structure. Finally, the proposed structure of **3** was further undoubtedly defined by the X-ray diffraction analysis (Figure 4).

The structure of **5** was finally determined by 1D and 2D NMR data (Figure 2) along with the data from a previously reported synthetic intermediate (He et al., 2015; Zhang et al., 2015), and it was purified from natural for the first time.

Compound **9** was named dehydrocyclopeptin (Hayashi et al., 1997; Ma et al., 2012). It was first isolated from *Penicillium cyclopium* (Framm et al., 1973), but the chemical shift assignments of some signals and the configuration of its double bond needed to be discussed. In the current report, HSQC and HMBC spectra (Figure 2) helped to provide the ¹H and ¹³C NMR data (Table 3), and X-ray diffraction analysis unambiguously built up an *E* configuration of the double bond (Figure 4).

The rest of the compounds, namely, **6**, **7**, **8,** and **10**, were determined to be pesimquinolone R; peniprequinolone; 4,5-dihydroxy-3,4-dihydro-3-methoxy-4-(4′-methoxyphenyl)-2(1*H*)-quinolinone; and tunicoidine F, respectively, through comparison of the corresponding spectroscopic data with the literature. Among them, we first reported the X-ray data for compounds **6**, **7,** and **9**.

The antimicrobial activity of compounds **1–10** was examined against *S. aureus*, *E. coli,* and *C. albicans* with chloramphenicol or ketoconazole as the positive control. As the results show in Table 4, compound **1** demonstrated an obvious antimicrobial effect, while **3** and **4** exhibited activity toward *S. aureus* and *E. coli*.

Conclusion

In summary, an OSMAC-based strategy applied to *P. raistrickii* of changing cultivation status from shaking fermentation to a static condition in a liquid medium expanded the alkaloidal SM diversity and thus induced the accumulation of four unreported alkaloids, including three *β*-carbolines (**1–3**) and one 2-quinolinone (**4**), along with one new natural compound 2-quinolinone (**5**) and five known

TABLE 4 Antimicrobial activity of compounds 1–10 (MIC µg/mL).

	1	2	3	4	5	6	7	8	9	10	Control
S. aureus	8.0	>200	50.0	12.5	>200	>200	>200	>200	>200	>200	3.50[a]
E. coli	5.0	>200	25.0	50.0	–	–	–	–	–	–	7.50[a]
C. albicans	2.0	–	>200	>200	–	–	–	>200	>200	>200	7.50[b]

[a]Chloramphenicol. [b]Ketoconazole. –, no activity.

alkaloids (**6**–**10**). The outcome indicated a big effect from a small change in the OSMAC strategy application, showing it to be a powerful tool in unlocking the fungal cryptic BGCs to obtain novel natural products.

β-Carboline alkaloids possess the fundamental framework of tricyclic pyrido [3,4-b] indole and are mainly obtained from plants and marine organisms, with only a few from microbes to our knowledge. 2-quinolinones, or named 2-quinolones, are quinoline derivatives with a carbonyl group inserted in the 2 position, most of which are produced by fungal genera (Neff et al., 2012). Benzodiazepine alkaloids are seven-membered cyclodipeptides composed of an anthranilic acid and another *α*-amino acid or its deoxygenated analogs. They are metabolites of filamentous fungi or actinomycetes, with one exception from sea hare up to now, and have not been found in higher plants (Roos, 1990; Ojika et al., 1993). These three kinds of alkaloids have a strong attraction to scientists due to their structural diversities and extensive scope of pharmacological effects, such as antitumor, antidepressant, antimicrobial, antimalarial, anti-inflammatory, antioxidant, insecticidal and analgesic effects (Roos, 1990; Cao et al., 2007; Cui et al., 2009; Wang et al., 2014; Simonetti et al., 2016; Reddy et al., 2018).

The structures of **1**–**10** were constructed by comprehensive analyses of the spectroscopic data. Measures including X-ray diffraction data, ECD, and optical rotation values helped to solve the absolute configurations of the new compounds. In addition, the configuration of the double band in compound **9** was unambiguously revised by X-ray diffraction data, and its ^{1}H and ^{13}C NMR data were reassigned in this work. Furthermore, it was the first report of the X-ray diffraction analyses on the absolute stereochemistry of compounds **7**.

All of the compounds (**1**–**10**) in the work were screened for their antimicrobial activity against microorganisms like *S. aureus*, *E. coli,* and *C. albicans*. Compounds **1**, **3,** and **4** showed antimicrobial effects. As for the *β*-carbolines obtained in the work, compound **1** exhibited an obvious pharmaceutical effect against tested microorganisms with MIC values of 8.0, 5.0, and 2.0 µg/mL, and compound **3** also showed some activity. The results implied that the amino acid residues and a free carboxyl group in this type of *β*-carboline alkaloids might play a pivotal part in the antimicrobial effect.

Data availability statement

The datasets generated for this study can be found in the online repositories. The names of the repository/repositories and accession number(s) can be found in the article/supplementary material.

Author contributions

MZ: Data curation, Investigation, Writing – original draft. HK: Investigation, Writing – original draft, Formal analysis. WL: Writing – original draft, Resources, Supervision, Validation, Visualization, Writing – review & editing. LM: Investigation, Writing – original draft, Formal analysis, Methodology. DL: Funding acquisition, Project administration, Supervision, Validation, Writing – review & editing.

Conflict of interest

The authors declare that the research was conducted in the absence of any commercial or financial relationships that could be construed as a potential conflict of interest.

Publisher's note

All claims expressed in this article are solely those of the authors and do not necessarily represent those of their affiliated organizations, or those of the publisher, the editors and the reviewers. Any product that may be evaluated in this article, or claim that may be made by its manufacturer, is not guaranteed or endorsed by the publisher.

Supplementary material

The Supplementary material for this article can be found online at: https://www.frontiersin.org/articles/10.3389/fmicb.2023.1279140/full#supplementary-material

References

Alexander, A. Z. (2023). Fungal BGCs for production of secondary metabolites: main types, central roles in strain improvement, and regulation according to the piano principle. *Int. J. Mol. Sci.* 24:11184. doi: 10.3390/ijms241311184

Belofsky, G. N., Gloer, K. B., Gloer, J. B., Wicklow, D. T., and Dowd, P. F. (1998). New p-terphenyl and polyketide metabolites from the sclerotia of *Penicillium raistrickii*. *J. Nat. Prod.* 61, 1115–1119. doi: 10.1021/np980188o

Bills, G. F., and Gloer, J. B. (2016). Biologically active secondary metabolites from the fungi. *Microbiol. Spectr.* 4, 1089–1119. doi: 10.1128/microbiolspec.FUNK-0009-2016

Bode, H. B., Bethe, B., Höfs, R., and Zeeck, A. (2002). Big effects from small changes: possible ways to explore nature's chemical diversity. *Chembiochem* 3, 619–627. doi: 10.1002/1439-7633(20020703)3:7<619::AID-CBIC619>3.0.CO;2-9

Cao, R. H., Peng, W. L., Wang, Z. H., and Xu, A. L. (2007). beta-Carboline alkaloids: biochemical and pharmacological functions. *Curr. Med. Chem.* 14, 479–500. doi: 10.2174/092986707779940998

Chen, Y. F., Kuo, P. C., Chan, H. H., Kuo, I. J., Lin, F. W., Su, C. R., et al. (2010). *β*-Carboline alkaloids from *Stellaria dichotoma var. lanceolata* and their anti-inflammatory activity. *J. Nat. Prod.* 73, 1993–1998. doi: 10.1021/np1003627

Cui, C. G., Li, X. M., Li, C. S., Sun, H. F., Gao, S. S., and Wang, B. G. (2009). Benzodiazepine alkaloids from marine-derived endophytic fungus *aspergillus ochraceus*. *Helv. Chim. Acta* 92, 1366–1370. doi: 10.1002/hlca.v92:7

Dai, C., Li, X., Zhang, K., Li, X. N., Wang, W., Zang, Y., et al. (2021). Pesimquinolones I-S, eleven new quinolone alkaloids produced by *Penicillium simplicissimum* and their inhibitory activity on NO production. *Bioorg. Chem.* 108:104635. doi: 10.1016/j.bioorg.2021.104635

Framm, J., Nover, L., El-Azzouny, A., Richter, H., Winter, K., Werner, S., et al. (1973). Cyclopeptin and dehydrocyclopeptin. Intermediates in the biosynthesis of cyclopeptin-viridicatin alkaloids in *Penicillium cyclopium* Westling. *Eur. J. Biochem.* 37, 78–85. doi: 10.1111/j.1432-1033.1973.tb02959.x

Genilloud, O. (2019). Natural products discovery and potential for new antibiotics. *Curr. Opin. Microbiol.* 51, 81–87. doi: 10.1016/j.mib.2019.10.012

Han, J. Y., Liu, M. M., Jenkins, I. D., Liu, X. T., Zhang, L. X., Quinn, R. J., et al. (2020a). Genome-inspired chemical exploration of marine fungus *Aspergillus fumigatus* MF071. *Mar. Drugs* 18:352. doi: 10.3390/md18070352

Han, J. Y., Zhang, J. Y., Song, Z. J., Zhu, G. L., Liu, M. M., Dai, H. Q., et al. (2020b). Genome-based mining of new antimicrobial meroterpenoids from the phytopathogenic fungus *Bipolaris sorokiniana* strain 11134. *Appl. Microbiol. Biotechnol.* 104, 3835–3846. doi: 10.1007/s00253-020-10522-1

Hayashi, H., Nakatani, T., Inoue, Y., Nakayama, M., and Nozaki, H. (1997). New dihydroquinolinone toxic to *artemia salina* produced by *Penicillium* sp. NTC-47. *Biosci. Biotechnol. Biochem.* 61, 914–916. doi: 10.1271/bbb.61.914

He, J., Lion, U., Sattler, I., Gollmick, F. A., Grabley, S., Cai, J. M., et al. (2015). Diastereomeric quinolinone alkaloids from the marine-derived fungus *Penicillium janczewskii*. *J. Nat. Prod.* 68, 1397–1399. doi: 10.1021/np058018g

Ishikawa, N., Tanaka, H., Koyama, F., Noguchi, H., Wang, C. C., Hotta, K., et al. (2014). Non-heme dioxygenase catalyzes atypical oxidations of 6, 7-bicyclic systems to form the 6, 6-quinolone core of viridicatin-type fungal alkaloids. *Angew. Chem. Int. Ed. Engl.* 53, 12880–12884. doi: 10.1002/anie.201407920

Jia, L. G., Dong, J. Z., Wang, R. J., Mao, S. H., Lu, F., Singh, S., et al. (2017). Identification and characterization of the steroid 15α-hydroxylase gene from *Penicillium raistrickii*. *Appl. Microbiol. Biotechnol.* 101, 6409–6418. doi: 10.1007/s00253-017-8377-3

Ke, J., and Yoshikuni, Y. (2020). Multi-chassis engineering for heterologous production of microbial natural products. *Curr. Opin. Biotechnol.* 62, 88–97. doi: 10.1016/j.copbio.2019.09.005

Li, J. L., Hu, Y. Y., Hao, X. M., Tan, J. L., Li, F., Qiao, X. R., et al. (2019). Raistrickindole a, an anti-hcv oxazinoindole alkaloid from *Penicillium raistrickii* IMB17-034. *J. Nat. Prod.* 82, 1391–1395. doi: 10.1021/acs.jnatprod.9b00259

Liu, D. S., Rong, X. G., Kang, H. H., Ma, L. Y., Hamann, M. T., and Liu, W. Z. (2018). Raistrickiones A-E from a highly productive strain of *Penicillium raistrickii* generated through thermo change. *Mar. Drugs* 16:213. doi: 10.3390/md16060213

Ma, L. Y., Liu, D. S., Li, D. G., Huang, Y. L., Kang, H. H., Wang, C. H., et al. (2016). Pyran rings containing polyketides from *Penicillium raistrickii*. *Mar. Drugs* 15:2. doi: 10.3390/md15010002

Ma, L. Y., Liu, W. Z., Shen, L., Huang, Y. L., Rong, X. G., Xu, Y. Y., et al. (2012). Spiroketals, isocoumarin, and indoleformic acid derivatives from saline soil derived fungus *Penicillium raistrickii*. *Tetrahedron* 68, 2276–2282. doi: 10.1016/j.tet.2012.01.054

Ma, L. Y., Zhang, H. B., Kang, H. H., Zhong, M. J., Liu, D. S., Ren, H., et al. (2019). New butenolides and cyclopentenones from saline soil-derived fungus aspergillus Sclerotiorum. *Molecules* 24:2642. doi: 10.3390/molecules24142642

Neff, S. A., Lee, S. U., Asami, Y., Ahn, J. S., Oh, H., Baltrusaitis, J., et al. (2012). Aflaquinolones A-G: secondary metabolites from marine and fungicolous isolates of *aspergillus* spp. *J. Nat. Prod.* 75, 464–472. doi: 10.1021/np200958r

Ojika, M., Yoshida, T., and Yamada, K. (1993). Aplysepine, a novel 1, 4-benzodiazepine alkaloid from the sea hare *Aplysia kurodai*. *Tetrahed. Lett.* 34, 5307–5308. doi: 10.1016/S0040-4039(00)73981-5

Palys, S., Pham, T. T. M., and Tsang, A. (2020). Biosynthesis of alkylcitric acids in *aspergillus Niger* involves both co-localized and unlinked genes. *Front. Microbiol.* 11:1378. doi: 10.3389/fmicb.2020.01378

Pan, R., Bai, X. L., Chen, J. W., Zhang, H. W., and Wang, H. (2019). Exploring structural diversity of microbe secondary metabolites using OSMAC strategy: a literature review. *Front. Microbiol.* 10:294. doi: 10.3389/fmicb.2019.00294

Reddy, T. R., Reddy, D. N., Reddy, B. K., Kasturaiah, C., and Yadagiri, K. (2018). An innovative approach for the synthesis of 7-hydroxyquinolin-2(1H)-one: a key intermediate of brexpiprazole. *Asian J. Chem.* 30, 834–836. doi: 10.14233/ajchem.2018.21092

Reen, F. J., Romano, S., Dobson, A. D., and O'Gara, F. (2015). The sound of silence: activating silent biosynthetic gene clusters in marine microorganisms. *Mar. Drugs* 13, 4754–4783. doi: 10.3390/md13084754

Romano, S., Jackson, S. A., Patry, S., and Dobson, A. D. W. (2018). Extending the "one strain many compounds" (OSMAC) principle to marine microorganisms. *Mar. Drugs* 16:244. doi: 10.3390/md16070244

Roos, W. (1990). *The alkaloids: Chemistry and pharmacology*. London: Academic Press_Series.

Sheldrick, G. M. (2014). *SHELXTL, version 5*.

Simonetti, S. O., Larghi, E. L., and Kaufman, T. S. (2016). Correction: a convenient approach to an advanced intermediate toward the naturally occurring, bioactive 6-substituted 5-hydroxy-4-aryl-1H-quinolin-2-ones. *Org. Biomol. Chem.* 14:3333. doi: 10.1039/c6ob90030e

Tangella, Y., Manasa, K. L., Krishna, N. H., Sridhar, B., Kamal, A., and Nagendra, B. (2018). Regioselective ring expansion of isatins with in *situ* generated α-aryldiazomethanes: direct access to viridicatin alkaloids. *Org. Lett.* 20, 3639–3642. doi: 10.1021/acs.orglett.8b01417

Uchida, R., Imasato, R., Yamaguchi, Y., Masuma, R., Shiomi, K., Tomoda, H., et al. (2006). Yaequinolones, new insecticidal antibiotics produced by *Penicillium* sp. FKI-2140. I. Taxonomy, fermentation, isolation and biological activity. *J. Antibiot. (Tokyo)* 59, 646–651. doi: 10.1038/ja.2006.86

Wang, K. B., Di, Y. T., Bao, Y., Yuan, C. M., Chen, G., Li, D. H., et al. (2014). Peganumine a, a β-carboline dimer with a new octacyclic scaffold from *Peganum harmala*. *Org. Lett.* 16, 4028–4031. doi: 10.1021/ol501856v

Wang, L., Zhang, X. Y., Zhang, K. J., Zhang, X. M., Zhu, T. J., Che, Q., et al. (2020). Overexpression of Global regulator Pbrlae a leads to the discovery of new polyketide in fungus *Penicillium Brocae* HDN-12-143. *Front. Chem.* 8:270. doi: 10.3389/fchem.2020.00270

Wen, B., Yuan, X., Zhang, W. D., Chen, B. Y., Fu, K. L., Li, B., et al. (2014). Chemical constituents from the aerial parts of *Psammosilene tunicoides*. *Phytochem. Lett.* 9, 59–66. doi: 10.1016/j.phytol.2014.04.006

Zhang, X., Hindra, , and Elliot, M. A. (2019). Unlocking the trove of metabolic treasures: activating silent biosynthetic gene clusters in bacteria and fungi. *Curr. Opin. Microbiol.* 51, 9–15. doi: 10.1016/j.mib.2019.03.003

Zhang, J. J., Tang, X. Y., and Moore, B. S. (2019). Genetic platforms for heterologous expression of microbial natural products. *Nat. Prod. Rep.* 36, 1313–1332. doi: 10.1039/c9np00025a

Zhang, Y. M., Wang, G., Lv, H. W., Luo, J. G., and Kong, L. Y. (2015). Two new β-carboline alkaloids from the roots of *Gypsophila oldhamiana*. *Nat. Prod. Res.* 29, 1207–1211. doi: 10.1080/14786419.2014.996755